Inorganic Chemistry

Article

# Characterization of a 1:1 Cu–O$_2$ Adduct Supported by an Anilido Imine Ligand

Anne M. Reynolds, Benjamin F. Gherman, Christopher J. Cramer,* and William B. Tolman*

Department of Chemistry, Center for Metals in Biocatalysis, and Supercomputer Institute, University of Minnesota, 207 Pleasant Street Southeast, Minneapolis, Minnesota 55455

Copper(I) complexes of sterically hindered anilido imine ligands $o\text{-}C_6H_4\{N(C_6H_3{}^iPr_2)\}\{C(R)\text{=}NC_6H_3{}^iPr_2\}^-$ (L^1, R = H; L^2, R = CH$_3$) have been prepared and characterized by spectroscopic and X-ray crystallographic methods. These complexes are highly reactive with O$_2$, and in the case of L^2 the product of low-temperature oxygenation was fully characterized by spectroscopic, X-ray crystallographic, and computational methods. The resonance Raman spectrum features an isotope-sensitive vibration at 974 cm^{-1} ($\Delta(^{18}O) = 66$ cm^{-1}), consistent with assignment as an O–O stretch. Despite the asymmetric coordination environment provided by the supporting anilido imine ligand, the X-ray crystal structure confirms rather symmetric side-on binding of the O$_2$ moiety to the copper center, and the O–O bond length of 1.392(2) Å indicates that this intermediate has significant Cu(III)–peroxo character. Theoretical calculations support this interpretation and predict that while a fully optimized end-on singlet geometry can be obtained, it is higher in energy than the side-on isomer by 3.5 kcal mol^{-1} at the CASPT2/TZP level.

Monocopper–dioxygen adducts have been postulated as intermediates in catalysis by enzymes, notable examples being dopamine β-monooxygenase,[1] peptidylglycine α-amidating monooxygenase,[2,3] and galactose oxidase.[4] Invariably formulated as Cu(II)–superoxo species, both end-on (η^1) and side-on (η^2) structures have been suggested for the
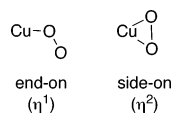
biological systems, although in only one instance has supporting evidence from X-ray crystallography been obtained.[2] How these intermediates compare in terms of electronic structure and reactivity is an unresolved issue in bioinorganic chemistry that serves as a significant objective for synthetic modeling studies.[5] A related goal is to understand how supporting ligands influence 1:1 Cu–O$_2$ adduct structures and properties.

While the end-on binding mode has been proposed for synthetic 1:1 Cu–O$_2$ adducts that have been identified kinetically,[6,7] spectroscopically,[8–10] and computationally,[10] none have been structurally characterized. Side-on coordination of O$_2$ to a variety of transition metals has been identified, with electronic structures that vary smoothly with respect to the degree of electron transfer to dioxygen between limiting superoxo and peroxo redox levels.[11,12] Only two examples of such side-on adducts with copper have been characterized by X-ray diffraction. A complex supported by a facially coordinating tris(pyrazolyl)hydroborate ligand was assigned as a Cu(II)–superoxo complex on the basis of spectroscopy

---

* To whom correspondence should be addressed. E-mail: cramer@chem.umn.edu (C.J.C.), tolman@chem.umn.edu (W.B.T.).

(1) Evans, J. P.; Ahn, K.; Klinman, J. P. *J. Biol. Chem.* **2003**, *278*, 49691.
(2) Prigge, S. T.; Eipper, B. A.; Mains, R. E.; Amzel, L. M. *Science* **2004**, *304*, 864.
(3) Chen, P.; Solomon, E. I. *J. Am. Chem. Soc.* **2004**, *126*, 4991.
(4) Whittaker, J. W. *Chem. Rev.* **2003**, *103*, 2347.
(5) (a) Mirica, L. M.; Ottenwaelder, X.; Stack, T. D. P. *Chem. Rev.* **2004**, *104*, 1013. (b) Lewis, E. A.; Tolman, W. B. *Chem. Rev.* **2004**, *104*, 1047.

(6) (a) Karlin, K. D.; Kaderli, S.; Zuberbühler, A. D. *Acc. Chem. Res.* **1997**, *30*, 139. (b) Fry, H. C.; Scaltrito, D. V.; Karlin, K. D.; Meyer, G. J. *J. Am. Chem. Soc.* **2003**, *125*, 11866.
(7) Schindler, S. *Eur. J. Inorg. Chem.* **2000**, 2311.
(8) Chaudhuri, P.; Hess, M.; Weyhermüller, T.; Wieghardt, K. *Angew. Chem., Int. Ed.* **1999**, *38*, 1095.
(9) Komiyama, K.; Furutachi, H.; Nagatomo, S.; Hashimoto, A.; Hayashi, H.; Fujinami, S.; Suzuki, M.; Kitagawa, T. *Bull. Chem. Soc. Jpn.* **2004**, *77*, 59.
(10) Schatz, M.; Raab, V.; Foxon, S. P.; Brehm, G.; Schneider, S.; Reiher, M.; Holthausen, M. C.; Sundermeyer, J.; Schindler, S. *Angew. Chem., Int. Ed.* **2004**, *43*, 4360.
(11) (a) Cramer, C. J.; Tolman, W. B.; Theopold, K. H.; Rheingold, A. L. *Proc. Natl. Acad. Sci. U.S.A.* **2003**, *100*, 3635 and references therein. (b) Hu, X.; Castro-Rodriguez, I.; Meyer, K. *J. Am. Chem. Soc.* **2004**, *126*, 13464. (c) Rahman, A. F. M. M.; Jackson, W. G.; Willis, A. C. *Inorg. Chem.* **2004**, *43*, 7558.
(12) Gherman, B. F.; Cramer, C. J. *Inorg. Chem.* **2004**, *43*, 7281.

and theory.[11a,13] We recently reported the synthesis and characterization of 1:1 Cu−O$_2$ adducts bearing sterically demanding β-diketiminate ligands.[14] An X-ray crystal structure of one confirmed a side-on binding mode, although severe disorder problems complicated detailed interpretation of structural data.[14b,c] Nonetheless, these parameters, in conjunction with theoretical and spectroscopic results, indicated significant Cu(III)−peroxide character for the adducts.[11,12,14]

Unfortunately, the β-diketiminate complexes are generally unreactive toward organic substrates,[15] suggesting the possible need for a less reduced O$_2$ moiety (i.e., more superoxo character) or for electrophilic activation of the peroxide-like ligand (e.g., by protons) to model functional aspects of the enzymes. The central methine position of the β-diketiminate ligand is known[16−18] to be susceptible to electrophilic attack, however, which complicates reactivity studies with electrophiles. We hypothesized that these issues could be addressed by using related anilido imine ligands L^1 (known[19]) and L^2 (yet to be reported) in which the potential for reactivity at

L^1 (R = H)
L^2 (R = CH$_3$)
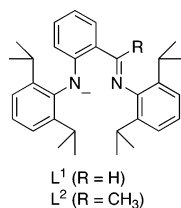
the central methine position of the backbone is eliminated by incorporation into the phenyl ring.[20] We also envisioned that the asymmetry of the ligand could potentially induce

asymmetry in the mode of dioxygen binding, perhaps even driving the O$_2$ to an end-on geometry via differential trans influences. Indeed, theoretical calculations on the mechanism of oxygenation of Cu(I) complexes of the β-diketiminate ligand revealed the involvement of a 3-coordinate end-on Cu(II)−superoxo species as a relatively low energy intermediate.[14c] To test these hypotheses, we targeted Cu(I) complexes of L^1 and L^2 for synthesis and undertook experimental and theoretical explorations of their reactivity with O$_2$, the results of which are reported herein. Key findings include a high-quality X-ray crystal structure of a new 1:1 Cu−O$_2$ adduct supported by L^2 and theoretical calculations that substantiate and augment the experimental results. Despite indications from crystallography of asymmetry in the binding of L^2 to Cu(I), the O$_2$ adduct exhibits side-on coordination akin to that seen previously in complexes with symmetric β-diketiminates, suggesting that further ligand manipulation will be required to stabilize the alternative end-on binding mode in low-coordinate compounds.

Experimental Section

General Considerations. All solvents and reagents were obtained from commercial sources and used as received unless otherwise stated. The solvents tetrahydrofuran (THF), diethyl ether (Et$_2$O), toluene, and pentane were passed through solvent purification columns (Glass Contour, Laguna, CA). Acetone was distilled twice from anhydrous calcium sulfate, and passed through a column of activated alumina immediately prior to use. Hexanes and deuterated benzene (C$_6$D$_6$) were distilled from Na/benzophenone. *n*-Butyllithium was titrated with diphenylacetic acid prior to use. 2,6-Diisopropylaniline was distilled from potassium hydroxide. All metal complexes were prepared and stored in a Vacuum Atmospheres inert atmosphere glovebox under a dry N$_2$ atmosphere or using standard Schlenk and vacuum line techniques. [Cu(CH$_3$CN)$_4$]-O$_3$SCF$_3$[21] and L^{1}Cu(MeCN)[16] were prepared via previously reported methods.

Physical Methods. NMR spectra were recorded on a Varian VI-300 or a VXR-300 spectrometer. Chemical shifts (δ) for ^{1}H and ^{13}C NMR spectra were referenced to residual protium in the deuterated solvent. UV−vis spectra were recorded on an HP8453 (190−1100 nm) diode array spectrophotometer. Low-temperature spectra were acquired using a Unisoku low-temperature UV−vis cell holder. Resonance Raman spectra were collected on an Acton AM-506 spectrometer using a Princeton Instruments LN/CCD-1100-PB/UVAR detector and ST-1385 controller interfaced with Winspec software, with 4 cm^{-1} spectral resolution. A Spectra Physics BeamLok 2060-KR-V krypton ion laser with a power of 50 mW at the sample was used to provide excitation at 406.7 nm. The spectra were obtained at 77 K using a backscattering geometry; samples were frozen onto a cold-plated copper coldfinger in thermal contact with a dewar containing liquid nitrogen. Raman shifts were externally referenced to liquid indene. High-resolution mass spectra were acquired on a Bruker BioTOF II ESI-TOF/MS using PEG-600 as an internal standard. X-band EPR spectra were acquired on a Bruker E-500 spectrometer, with an Oxford Instruments EPR-10 liquid helium cryostat (4−20 K, 9.61 GHz). Elemental analyses were performed by Atlantic Microlabs of Norcross, GA.

(13) (a) Fujisawa, K.; Tanaka, M.; Moro-oka, Y.; Kitajima, N. *J. Am. Chem. Soc.* **1994**, *116*, 12079. (b) Chen, P.; Root, D. E.; Campochiaro, C.; Fujisawa, K.; Solomon, E. I. *J. Am. Chem. Soc.* **2003**, *125*, 466.

(14) (a) Spencer, D. J. E.; Aboelella, N. W.; Reynolds, A. M.; Holland, P. L.; Tolman, W. B. *J. Am. Chem. Soc.* **2002**, *124*, 2108. (b) Aboelella, N. W.; Lewis, E. A.; Reynolds, A. M.; Brennessel, W. W.; Cramer, C. J.; Tolman, W. B. *J. Am. Chem. Soc.* **2002**, *124*, 10660. (c) Aboelella, N. W.; Kryatov, S. V.; Gherman, B. F.; Brennessel, W. W.; Young, V. G., Jr.; Sarangi, R.; Rybak-Akimova, E. V.; Hodgson, K. O.; Hedman, B.; Solomon, E. I.; Cramer, C. J.; Tolman, W. B. *J. Am. Chem. Soc.* **2004**, *126*, 16896.

(15) Reynolds, A. M.; Lewis, E. A.; Aboelella, N. W.; Tolman, W. B. *Chem. Commun.* **2005**, 2014.

(16) Brown, E. C.; Aboelella, N. W.; Reynolds, A. M.; Aullón, G.; Alvarez, S.; Tolman, W. B. *Inorg. Chem.* **2004**, *43*, 3335.

(17) Jazdzewski, B. A.; Holland, P. L.; Pink, M.; Young, V. G., Jr.; Spencer, D. J. E.; Tolman, W. B. *Inorg. Chem.* **2001**, *40*, 6097.

(18) (a) Yokota, S.; Tachi, Y.; Itoh, S. *Inorg. Chem.* **2002**, *41*, 1342. (b) Basuli, F.; Huffman, J. C.; Mindiola, D. J. *Inorg. Chem.* **2003**, *42*, 8003. (c) Radzewich, C. E.; Coles, M. P.; Jordan, R. F. *J. Am. Chem. Soc.* **1998**, *120*, 9384. (d) Fekl, U.; Kaminsky, W.; Goldberg, K. I. *J. Am. Chem. Soc.* **2001**, *123*, 6423. (e) Ragogna, P. J.; Burford, N.; D'eon, M.; McDonald, R. *Chem. Commun.* **2003**, 1052. (f) Hitchcock, P. B.; Lappert, M. F.; Nycz, J. E. *Chem. Commun.* **2003**, 1142. (g) Carey, D. T.; Cope-Eatough, E. K.; Vilaplana-Mafé, E.; Mair, F. S.; Pritchard, R. G.; Warren, J. E.; Woods, R. J. *Dalton Trans.* **2003**, 1083.

(19) Hayes, P. G.; Welch, G. C.; Emslie, D. J. H.; Noack, C. L.; Piers, W. L.; Parvez, M. *Organometallics* **2003**, *22*, 1577.

(20) Ligands related to L^1 and L^2 have been reported: (a) Porter, R. M.; Winston, S.; Danopoulos, A. A.; Hursthouse, M. B. *J. Chem. Soc., Dalton Trans.* **2002**, 3290. (b) Porter, R. M.; Danopoulos, A. A. *Dalton Trans.* **2004**, 2556. (c) Gao, H.; Guo, W.; Bao, F.; Gui, G.; Zhang, J.; Zhu, F.; Wu, Q. *Organometallics* **2004**, *23*, 6273. (d) Liu, X.; Gao, W.; Mu, Y.; Li, G.; Ye, L.; Xia, H.; Ren, Y.; Feng, S. *Organometallics* **2005**, *24*, 1614.

(21) Kubas, G. J. *Inorg Synth.* **1979**, *19*, 90.

o-C₆H₄(C(CH₃)=NC₆H₃ⁱPr₂-2,6). A solution of TiCl₄ (1.45 mL, 0.0133 mol) in hexanes (10 mL) was slowly added to a solution of 2,6-diisopropylaniline (15 mL, 0.0795 mol) in hexanes (75 mL) at 0 °C under N₂, causing the formation of a dense brown precipitate. The mixture was stirred for 2 h at 0 °C and then warmed to room temperature. 2′-Fluoroacetophenone (3.4 mL, 0.0265 mol) was then added via syringe, causing the brown color to lighten slightly. The mixture was then heated to reflux overnight. The resultant yellow mixture was cooled to room temperature, and 100 mL of Et₂O was added. After being stirred for 15 min, the mixture was filtered on a frit, and the filter cake was washed with Et₂O (50 mL). The volume of the solution was reduced to ∼50 mL total, and this was filtered through Celite to remove the remaining precipitates. The solvent was removed under reduced pressure to yield an orange-brown oil. Column chromatography on silica gel (90% hexanes, 10% ethyl acetate; R_f = 0.35) afforded the clean imine. Total yield: 4.51 g (57%). ¹H NMR (300 MHz, CDCl₃): δ 7.92 (td, J = 7.8, 1.8 Hz, 1H), 7.45 (dddd, J = 8.1, 7.4, 5.1, 1.8 Hz, 1H), 7.30−7.09 (m, 5H), 2.86 (sept, J = 6.9 Hz, 2H), 2.15 (d, $J_{H,F}$ = 3.3 Hz, 3H), 1.24 (d, J = 6.9 Hz, 6H), 1.23 (d, J = 6.9 Hz, 6H) ppm. ¹³C NMR (75 MHz, CDCl₃): δ 165.08 (d, $J_{C,F}$ = 2 Hz), 161.21 (d, $J_{C,F}$ = 249 Hz), 145.95, 136.31, 131.59 (d, $J_{C,F}$ = 8 Hz), 130.08 (d, $J_{C,F}$ = 4 Hz), 128.74 (d, $J_{C,F}$ = 13 Hz), 124.58 (d, $J_{C,F}$ = 3 Hz), 123.88, 123.21, 116.46 (d, $J_{C,F}$ = 23 Hz), 28.34, 23.55, 23.16, 21.83 (d, $J_{C,F}$ = 6 Hz, CH₃) ppm. Anal. Calcd for C₂₀H₂₄FN: C, 80.77; H, 8.13; N, 4.71. Found: C, 80.84; H, 8.17; N, 4.80.

o-C₆H₄{NH(C₆H₃ⁱPr₂)}{C(CH₃)=NC₆H₃ⁱPr₂} (L²H). *n*-BuLi in hexanes (6.3 mL, 0.0164 mol) was slowly added to a solution of 2,6-diisopropylaniline (3.2 mL, 0.0171 mol) in THF (40 mL), at −78 °C. The solution was allowed to slowly warm to room temperature and was then added to a solution of o-C₆H₄(C(CH₃)=NC₆H₃ⁱPr₂-2,6) (4.43 g, 0.0149 mol) in ∼10 mL of THF, causing a color change to deep red. The solution was then heated to reflux under N₂ for 36 h. After being cooled to room temperature, the reaction was quenched with H₂O (50 mL) and extracted with hexanes (100 mL). The aqueous layer was washed with 2 × 50 mL of hexanes, and the organics were combined, dried over Na₂SO₄, and evaporated to dryness to yield an orange oily solid. This was dissolved in hot ethanol (200 mL) and slowly cooled to −20 °C to yield yellow crystals that were filtered, washed with cold EtOH (50 mL), and dried under vacuum. Concentration of the mother liquor and cooling to −20 °C yielded a second crop of crystals. Total yield: 3.10 g (46%). ¹H NMR (300 MHz, CDCl₃): δ 11.29 (s, 1H), 7.75 (dd, 1H, J = 8.1, 1.5 Hz), 7.20 (m, 7H), 6.80 (td, 1H, J = 7.5, 1.2 Hz), 6.30 (dd, 1H, J = 8.4, 0.9 Hz), 3.23 (sept, 2H, J = 6.9 Hz), 2.93 (sept, 2H, J = 6.9 Hz), 2.26 (s, 3H), 1.17 (d, J = 6.9 Hz, 6H), 1.14 (d, J = 6.9 Hz, 6H), 1.12 (d, J = 6.9 Hz, 6H), 1.11 (d, J = 6.9 Hz, 6H) ppm. ¹³C NMR (75 MHz, CDCl₃): δ 145.40, 137.16, 135.04, 131.79, 130.69, 127.38, 123.98, 123.29, 117.28, 114.59, 113.26, 28.63, 28.40, 24.73, 23.87, 23.74, 23.53, 19.33 ppm. HREIMS: m/z calcd for C₃₂H₄₂N₂ ([M + H]⁺), 455.3426; found, 455.3432.

L²Li. *n*-BuLi (0.47 mL, 1.21 mmol) was slowly added to a solution of L²H (0.50 g, 1.10 mmol) in toluene (4 mL). The yellow solution was stirred for 15 min, and the solvent was slowly removed in vacuo, yielding a yellow powder. Pentane (3 mL) was added, and the mixture was stored at −20 °C overnight. The product was then filtered, washed with cold pentane (5 mL), and dried under vacuum. Yield: 0.44 g (86%). ¹H NMR (300 MHz, C₆D₆): δ 7.61 (dd, J = 8.4, 1.5 Hz, 1H), 7.28 (m, 3 H), 7.19 (m, 3H), 7.01 (ddd, J = 8.9, 6.6, 1.8 Hz, 1H), 6.53 (dd, J = 8.7, 1.5 Hz, 1H), 6.34 (ddd, J = 8.3, 6.6, 1.5 Hz, 1H), 3.27 (sept, 2H, J = 6.9 Hz), 2.73 (sept, 2H, J = 6.9 Hz), 2.05 (s, 3H), 1.20 (d, 6H, J = 6.9 Hz),

1.16 (d, 6H, J = 6.9 Hz), 1.05 (d, 6H, J = 6.9 Hz), 1.00 (d, 6H, J = 6.9 Hz) ppm. ¹³C NMR (75 MHz, C₆D₆): δ 170.35, 158.84, 150.47, 147.43, 143.22, 139.15, 133.96, 132.38, 124.96, 124.28, 123.18, 118.94, 116.74, 109.44, 103.56, 28.73, 28.50, 25.58, 24.71, 24.20, 24.07, 21.22 ppm.

L²Cu(MeCN). A solution of L²Li (0.59 g, 1.30 mmol) in THF (5 mL) was added to a slurry of [Cu(CH₃CN)₄]O₃SCF₃ (0.48 g, 1.30 mmol) in THF (1 mL), causing the development of a red-orange color. After the resulting solution was stirred for 15 min, the solvent was slowly removed in vacuo. Toluene (10 mL) was added, and the mixture was stirred for 10 min and then filtered through Celite. The volume was reduced to 2 mL under vacuum, and 6 mL of pentane was added. Storage at −20 °C led to the deposition of orange crystals, which were isolated, washed with cold pentane (2 mL), and dried under vacuum. Yield: 0.149 g (21%). ¹H NMR (300 MHz, C₆D₆): δ 7.67 (dd, J = 8.4, 1.5 Hz, 1H), 7.34 (m, 2 H), 7.21 (dd, J = 7.7, 1.5 Hz, 1H), 7.06 (m, 4H), 6.75 (dd, J = 9.0, 1.5 Hz, 1H), 6.42 (ddd, J = 8.3, 6.6, 1.5 Hz, 1H), 3.70 (sept, 2H, J = 6.9 Hz), 3.23 (sept, 2H, J = 6.9 Hz), 2.13 (s, 3H), 1.43 (d, 6H, J = 6.9 Hz), 1.30 (d, 6H, J = 6.9 Hz), 1.27 (d, 6H, J = 6.9 Hz), 1.14 (d, 6H, J = 6.9 Hz) ppm. ¹³C NMR (75 MHz, C₆D₆): δ 169.09, 158.29, 150.00, 147.70, 142.81, 138.80, 133.89, 132.17, 124.43, 124.32, 123.89, 123.64, 118.99, 115.06, 110.97, 28.77, 28.43, 25.14, 24.67, 24.57, 23.94, 21.42, 0.41 ppm. UV−vis (THF, −80 °C) [λ_{max}, nm (ϵ, M⁻¹ cm⁻¹)]: 440 (11700), 453 (12000). Anal. Calcd for C₃₄H₄₄CuN₃: C, 73.15; H, 7.94; N, 7.53. Found: C, 72.52; H, 7.86; N, 7.32.

Characterization Data for L²CuO₂. UV−vis (THF, −80 °C) [λ_{max}, nm (ϵ, M⁻¹ cm⁻¹)]: 390 (sh, 7600), 440 (10300), 453 (11300), 650 (200). Resonance Raman (λ_{ex} = 406.7 nm, 77 K, acetone): 908 (¹⁸O₂), 974 (¹⁶O₂) cm⁻¹. EPR (THF, 20 K, 9.60 GHz): silent.

X-ray Crystallography. Crystals of the appropriate size were placed onto the tip of a 0.1 mm diameter glass capillary and mounted on a Bruker SMART Platform CCD diffractometer for data collection at 173(2) K. (In the case of L²CuO₂, the crystals were mounted from a cold nitrogen platform at −80 °C.) Data collections were carried out using Mo Kα radiation (graphite monochromator) with a detector distance of 4.9 cm. A randomly oriented region of reciprocal space was surveyed to the extent of 1.5 hemispheres and to a resolution of 0.84 Å. Three major sections of frames were collected with 0.30° steps in ω at three different φ settings and at a detector position of −28° in 2θ. The intensity data were corrected for absorption and decay (SADABS).²² Final cell constants were calculated from the *xyz* centroids of strong reflections from the actual data collection after integration (SAINT).²³ Additional crystal and refinement information is presented in the CIFs (Supporting Information).

The structures were solved by direct methods using SIR97,²⁴ which located most non-hydrogen atoms from the e-map. Full-matrix least-squares/difference Fourier cycles were performed using SHELXL-97,²⁵ which located the remaining non-hydrogen atoms. The space groups $P2_1/c$ for L²Cu(MeCN) and $C2/c$ for L²CuO₂, respectively, were determined on the basis of systematic absences and intensity statistics. All non-hydrogen atoms were refined with

(22) An empirical correction for absorption anisotropy: Blessing, R. *Acta Crystallogr.* **1995**, *A51*, 33.
(23) *SAINT V6.2*; Bruker Analytical X-Ray Systems: Madison, WI, 2001.
(24) Altomare, A.; Burla, M. C.; Camalli, M.; Cascarano, G.; Giacovazzo, C.; Guagliardi, A.; Moliterni, A. G. G.; Polidori, G.; Spagna, R. Sir97: a new tool for crystal structure determination and refinement. *J. Appl. Crystallogr.* **1998**, *32*, 115.
(25) *SHELXTL V6.10*; Bruker Analytical X-Ray Systems: Madison, WI, 2000.

anisotropic displacement parameters. All hydrogen atoms were placed in ideal positions and refined as riding atoms with relative isotropic displacement parameters. Pertinent details for each structure are noted below; see the CIFs (Supporting Information) for full crystallographic information.

(A) L²Cu(MeCN). Crystals suitable for X-ray crystallography were grown at −20 °C from a mixture of toluene and pentane. The terminal methyl group of the bound acetonitrile moiety has a high thermal parameter, indicating possible disorder. Repeated attempts to model this disorder did not lead to an improvement in the overall model, and were thus abandoned. The final full-matrix least-squares refinement converged to R1 = 0.0369 and wR2 = 0.1037 (F^2, all data).

(B) L²CuO₂. Crystals suitable for X-ray crystallography were grown at −80 °C from a solution of the complex, which was generated by bubbling O₂ through a solution of L²Cu(MeCN) in a mixture of Et₂O, pentane, and acetone (49:49:2, v/v/v) at −80 °C. Solvent molecules were found in channels along the *b*-axis of the crystal, but they could not be satisfactorily modeled. To obtain a better model, the solvent molecules were removed using the program PLATON, function SQUEEZE,[26] from which it was determined that there were 219 electrons in a volume of 1162 Å³, out of a unit cell volume of 6752 Å³ (17.2%). There are weak hydrogen-bonding interactions between the oxygen atoms of the O₂ moiety and aromatic C−H bonds of neighboring molecules. O1 lies 2.537 Å from H1 of another molecule, while O2 lies 2.397 Å from H24 of a different molecule. The final full-matrix least-squares refinement converged to R1 = 0.0446 and wR2 = 0.1102 (F^2, all data).

Computational Design. (A) DFT Methods. Geometry optimizations were carried out on Cu complexes of the full ligand L² using the Jaguar suite, version 5.0, of ab initio quantum chemistry programs.[27] Calculations used DFT with the B3LYP functional,[28−30] a restricted (RDFT) methodology for the singlet cases, and an unrestricted (UDFT) methodology for the triplet cases. Such a procedure was found to be optimal for generating minimum energy structures in earlier studies modeling 1:1 Cu−O₂ adducts supported by β-diketiminate ligands.[12,14c] The LACVP** basis set, which includes an effective core potential and a double-ζ plus polarization (DZP) basis set for the valence electrons, was used for Cu.[31] The DZP 6-31G** basis set was used for all other atoms.

Vibrational frequencies were calculated analytically using, for computational tractability, a truncated ligand L³ obtained by replacing the isopropyl groups from L² with hydrogen atoms and
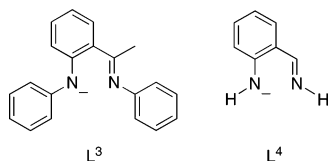
optimizing the positions of these capping H atoms with the remainder of the structure held fixed. These calculations verified

the B3LYP/DZP-optimized structures as stationary points and allowed for zero-point energy, enthalpy, and entropy corrections to be made and consequently for free energies to be obtained. Subsequently, minima were reoptimized with B3LYP using a triple-ζ plus polarization (TZP) basis set, namely, 6-311G**, for all atoms except Cu, for which the LACV3P** basis set (a triple-ζ basis compatible with the effective core potential) was used.[31] Reported O−O stretching frequencies for the truncated models were assessed at this level[11a] following scaling by a factor of 0.97.[32]

(B) Multireference Methods. Adducts of Cu(I) complexes and dioxygen may possess some degree of Cu(II)−superoxide character. Considering that Cu(II)−superoxide is formally a biradical with one electron localized on Cu and another on the O₂ moiety, and that such an open-shell singlet state cannot be formally expressed in a single determinantal framework (such as Kohn−Sham DFT), multireference methods must be used to calculate accurate energies for these adducts, particularly for the purpose of predicting state-energy splittings. To this end, single-point calculations using multireference second-order perturbation theory (CASPT2)[33] were performed using MOLCAS.[34] These calculations used a polarized valence triple-ζ atomic natural orbital basis set for O, N, and H (N−H) atoms,[35] 3-21G for C atoms,[36] STO-3G for all other H atoms,[37] and a 17-electron relativistic effective core potential for Cu with a TZP basis set for the valence electrons.[38] In initial calculations, the complete active space for the reference wave function consisted of 18 electrons and 12 orbitals comprised from the Cu valence electrons/orbitals and the σ_{2p}, σ_{2p}^*, π_{2p}, and π_{2p}^* electrons/orbitals of O₂. By removing orbitals found to have occupation numbers greater than 1.999, a final (12,9) subspace was obtained.

For calculations at this level of theory to be tractable, the CASPT2 calculations were carried out on a simplified version of the anilido imine ligand system (L⁴) in which the backbone methyl group and the 2,6-diisopropylphenyl flanking groups were changed to hydrogen atoms. The difference between the singlet−triplet energy splitting at the DFT and CASPT2 levels for L⁴CuO₂ was calculated according to eq 1. Assuming the triplet to be well-
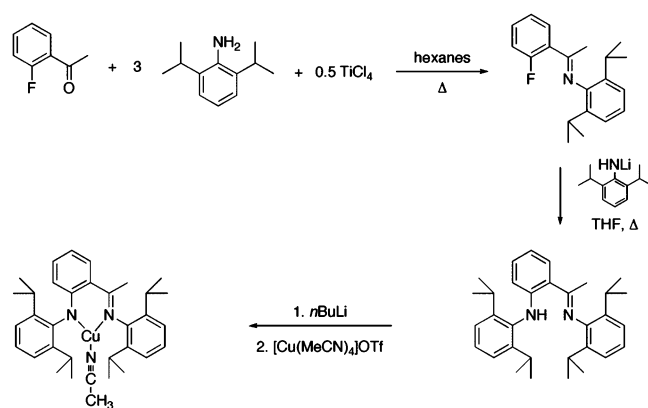
$$\Delta = (^1A - {}^3A)_{\text{CASPT2}} - (^1A - {}^3A)_{\text{DFT}} = [(^1A)_{\text{CASPT2}} - (^1A)_{\text{DFT}}] - [(^3A)_{\text{CASPT2}} - (^3A)_{\text{DFT}}] \quad (1)$$

described by a single-determinantal method such as DFT, the relative energy difference for the triplet between the two levels of theory is zero. Equation 1 then reduces to the relative difference in singlet energies from DFT and CASPT2 and can be interpreted as giving a CASPT2-based energy correction to the singlet energy obtained from DFT. Combining this "CASPT2 correction" with the DFT energies obtained for L² yields final electronic energies for the 1:1 Cu−O₂ adducts with the full ligand system.

(26) Spek, A. L. *Acta Crystallogr.* **1990**, *A46*, C34. Spek, A. L. *PLATON, A Multipurpose Crystallographic Tool*; Utrecht University: Utrecht, The Netherlands, 2000.
(27) *Jaguar 5.0*; Schrodinger, LLC: Portland, OR, 2002.
(28) Johnson, B. G.; Gill, P. M. W.; Pople, J. A. *J. Chem. Phys.* **1993**, *98*, 5612.
(29) Becke, A. D. *J. Chem. Phys.* **1993**, *98*, 1372.
(30) Lee, C. T.; Yang, W. T.; Parr, R. G. *Phys. Rev. B* **1988**, *37*, 785.
(31) (a) Hay, P. J.; Wadt, W. R. *J. Chem. Phys.* **1985**, *82*, 270. (b) Wadt, W. R.; Hay, P. J. *J. Chem. Phys.* **1985**, *82*, 284. (c) Hay, P. J.; Wadt, W. R. *J. Chem. Phys.* **1985**, *82*, 299.

(32) Bauschlicher, C. W.; Partridge, H. *J. Chem. Phys.* **1995**, *103*, 1788.
(33) Andersson, K.; Malmqvist, P. A.; Roos, B. O. *J. Chem. Phys.* **1992**, *96*, 1218.
(34) Karlstrom, G.; Lindh, R.; Malmqvist, P. A.; Roos, B. O.; Ryde, U.; Veryazov, V.; Widmark, P. O.; Cossi, M.; Schimmelpfennig, B.; Neogrady, P.; Seijo, L. *Comput. Mater. Sci.* **2003**, *28*, 222.
(35) Pierloot, K.; Dumez, B.; Widmark, P. O.; Roos, B. O. *Theor. Chim. Acta* **1995**, *90*, 87.
(36) Binkley, J. S.; Pople, J. A.; Hehre, W. J. *J. Am. Chem. Soc.* **1980**, *102*, 939.
(37) Hehre, W. J.; Stewart, R. F.; Pople, J. A. *J. Chem. Phys.* **1969**, *51*, 2657.
(38) Barandiaran, Z.; Seijo, L. *Can. J. Chem.* **1992**, *70*, 409.

Scheme 1

Figure 1. UV−vis absorption spectra of THF solutions of $L^2Cu(MeCN)$ (dashed line) and the product of its oxygenation (solid line) at −80 °C.

Results and Discussion

Synthesis and Characterization of Cu(I) Complexes. The complex $L^1Cu(MeCN)$ was prepared from L^1Li and $[Cu(MeCN)_4]O_3SCF_3$ and was structurally characterized by X-ray diffraction, as described elsewhere.[16] The ligand precursor L^2H was synthesized in two steps, in a manner similar to that previously reported for L^1H,[19] with some modifications (Scheme 1). The initial condensation of 2,6-diisopropylaniline with 2′-fluoroacetophenone to form the imine did not proceed to an appreciable extent by typical acid-catalyzed condensation procedures. However, reasonable yields were obtained by adding 2′-fluoroacetophenone to a preformed mixture of $TiCl_4$ and 2,6-diisopropylaniline, followed by refluxing overnight.[18g,39] The second step requires nucleophilic aromatic substitution of the fluorine using the lithium salt of 2,6-diisopropylaniline. While this reaction proceeded readily at ambient temperatures for L^1H,[19] elevated temperatures were required to form L^2H, which was then fully characterized by ^1H and ^{13}C NMR spectroscopy and high-resolution mass spectrometry. Deprotonation with *n*-butyllithium in toluene yielded the lithium salt L^2Li as a bright yellow powder. Finally, the lithium salt was treated with $[Cu(MeCN)_4]O_3SCF_3$ to form the copper(I) complex $L^2Cu(MeCN)$, which was isolated as red-orange crystals. This deep coloration is due to an intense absorption band at 450 nm ($\epsilon \approx 12000$ M^{-1} cm^{-1}; Figure 1, dashed line), which most likely is a ligand-based $\pi−\pi^*$ transition that is red-shifted relative to the corresponding feature[40] observed for Cu(I) complexes of β-diketiminate ligands ($\lambda_{max} \approx 380$ nm, $\epsilon \approx 20\,000$ M^{-1} cm^{-1}).[41]

The X-ray crystal structure of $L^2Cu(MeCN)$ is shown alongside the previously reported structure for $L^1Cu(MeCN)$ in Figure 2a,b; selected bond distances and angles and crystallographic data are listed in Tables 1 and S1 (Supporting Information), respectively. Despite gross similarities between them, several important differences are apparent.
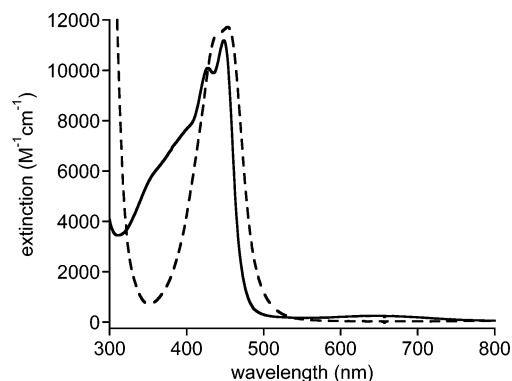
For example, the $C_\alpha−N_{imine}−C_{aryl}$ angle in the complex of L^2 is 122.2(2)°, whereas in $L^1Cu(MeCN)$ it is 113.0(5)°, signifying greater steric hindrance about the ligand binding pocket of the former that is induced by the backbone methyl group. Analogous influences of the backbone substitution pattern have been noted in other β-diketiminate complexes.[14,41,42] Another difference between the structures concerns the coordinated MeCN ligand, which is bound symmetrically between the Cu−N bonds in the complex of L^1, but displaced to one side in the complex of L^2 (the difference in the $N_{ligand}−Cu−N_{MeCN}$ angles is 36°). There is also significant asymmetry in the binding of L^2 to the copper center in the complex, with the difference in Cu−N bond distances $\Delta_{Cu−N} \cong 0.12$ Å; a lesser degree of asymmetry is present in $L^1Cu(MeCN)$ ($\Delta_{Cu−N} \cong 0.03$ Å). Significant asymmetry was reported for yttrium complexes of L^1 ($\Delta_{Y−N} \cong 0.13−0.16$ Å),[19] an effect that was attributed to localization of negative charge on the anilido nitrogen. In the case of $L^2Cu(MeCN)$, however, crystal packing effects may also contribute to the displaced geometry of the nitrile ligand and/or the Cu−N asymmetry. This is apparent from the crystal packing diagram (Figure S1 in the Supporting Information), where a hydrogen atom (H34B) on the bound acetonitrile lies 2.22 Å from a hydrogen atom on an isopropyl carbon from a neighboring molecule (H18A), thus indicating van der Waals contact that may underly the observed canting of the acetonitrile from the more symmetric position.[43] DFT calculations support attribution of this distortion to crystal packing effects. For example, in the minimum energy gas-phase structure (Figure 2c), the geometry is much closer to trigonal planar, with a difference in $N_{ligand}−Cu−N_{MeCN}$ angles ($\Delta_{N−Cu−N}$) of only 5.68° and a smaller $\Delta_{Cu−N} = 0.067$ Å. Rotation of the MeCN ligand to a more angled coordination by increasing $\Delta_{N−Cu−N}$ to ~35° leads to a structure only ~1.5 kcal mol^{-1} higher in energy. This small energy difference indicates that the displacement of the MeCN group in the

(39) Clegg, W.; Coles, S. J.; Cope, E. K.; Mair, F. S. *Angew. Chem., Int. Ed.* **1998**, *37*, 796.
(40) Randall, D. W.; DeBeer, S.; Holland, P. L.; Hedman, B.; Hodgson, K. O.; Tolman, W. B.; Solomon, E. I. *J. Am. Chem. Soc.* **2000**, *122*, 11632.
(41) Spencer, D. J. E.; Reynolds, A. M.; Holland, P. L.; Jazdzewski, B. A.; Duboc-Toia, C.; Le Pape, L.; Yokota, S.; Tachi, Y.; Itoh, S.; Tolman, W. B. *Inorg. Chem.* **2002**, *41*, 6307.

(42) Smith, J. M.; Lachicotte, R. J.; Holland, P. L. *Chem. Commun.* **2001**, 1542.
(43) It should also be noted that, in the crystal structure, the terminal methyl group of the acetonitrile moiety has a high thermal parameter, indicating possible disorder. However, attempts to model this disorder revealed that the two disordered components lie very close to one another with little effect on the overall acetonitrile coordination geometry. In any case, since these efforts did not lead to any improvement in the overall model, they were abandoned.
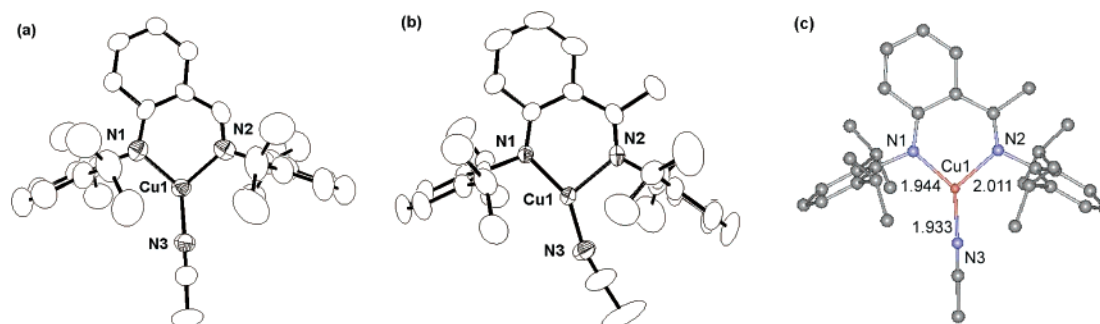
Figure 2. X-ray crystal structures of (a) L¹Cu(MeCN)[16] and (b) L²Cu(MeCN), alongside (c) the theoretically calculated structure for L²Cu(MeCN). In the X-ray structures, all non-hydrogen atoms are shown as 50% thermal ellipsoids. In the theoretical structure, hydrogen atoms are omitted for clarity, selected bond distances (Å) are reported, and gray represents C, blue N, red O, and pink Cu.

Table 1. Selected Interatomic Distances (Å) and Angles (deg)[a]

	L¹Cu(MeCN)[b]		
Cu−N1	1.926(4)	Cu−N2	1.951(4)
Cu−N3	1.859(4)	N1−Cu−N2	97.67(17)
N1−Cu−N3	134.88(17)	N2−Cu−N3	127.45(17)
C5−N1−C9	122.3(5)	C7−N2−C21	113.0(5)
	L²Cu(MeCN)		
Cu−N1	1.8829(17)	Cu−N2	2.0053(19)
Cu−N3	1.851(2)	N1−Cu−N2	94.79(8)
N1−Cu−N3	150.70(9)	N2−Cu−N3	114.49(9)
C5−N1−C9	118.97(18)	C7−N2−C21	122.2(2)
	L²CuO₂		
Cu−N1	1.828(2)	Cu−N2	1.865(2)
Cu−O1	1.821(2)	Cu−O2	1.831(2)
O1−O2	1.392(3)	N1−Cu−N2	98.59(10)
O1−Cu−O2	44.81(8)	N1−Cu−O1	107.61(9)
N2−Cu−O2	108.98(9)		

[a] Estimated standard deviations in parentheses. [b] This structure has been reported previously.[16] Atom numbers have been changed from those of the original structure to facilitate comparison.

plane of the ligand is a very soft mode, as would be expected for solvent ligation at such a Cu(I) center. Thus, while there is asymmetry present in the crystal structure of L²Cu(MeCN), it is not clear that this is an intrinsic property present in environments other than the crystalline state (e.g., in solution).

Dioxygen Reactivity (Experiment). Both L¹Cu(MeCN) and L²Cu(MeCN) are highly reactive with dioxygen both in solution and in the solid state, immediately developing a dark brown color when exposed to O₂ at room temperature. When the oxygenations are performed at low temperatures, intermediates are observed. In the case of L¹Cu(MeCN), at low concentrations in THF (∼0.2 mM), exposure to O₂ at −80 °C causes a color change to yellow-green. The UV−vis spectrum of this species is quite similar to that of the oxygenated product of L²Cu(MeCN) (vide infra). However, at higher concentrations such as those required for characterization by resonance Raman spectroscopy or for crystallization (>2 mM), THF solutions immediately turn dark brown on exposure to O₂ at −80 °C, and the spectral features do not change upon warming to room temperature. In acetone at higher concentrations (15 mM), solutions turn yellow-green when oxygenated at −80 °C, but if Ar is subsequently bubbled through the solution, a brown color develops. The spectral features of this brown solution also do not change upon warming. Thus, the formation of the yellow-green intermediate seems to be dependent on the solvent, concen-

tration, and presence of excess O₂, thus making characterization difficult and leading us to focus instead on the species derived from L²Cu(MeCN).

The UV−vis spectrum of the yellow-green intermediate resulting from oxygenation of L²Cu(MeCN) at −80 °C in THF, acetone, toluene, or diethyl ether (THF spectrum shown in Figure 1, solid line) is devoid of features that are characteristic of bis(μ-oxo)- or peroxodicopper intermediates.[5] Instead, it resembles UV−vis spectra of 1:1 Cu−O₂ adducts of the β-diketiminate ligands,[14a,c] with an intense shoulder at 390 nm (ε ≈ 7600) and a weaker band at 645 nm (ε ≈ 250). The spectral features of this EPR-silent intermediate did not decay upon bubbling of Ar through the solution, indicating that the oxygenation is irreversible under these conditions. Upon being warmed to room temperature, the solutions turn brown, consistent with decomposition. The EPR spectrum of the decomposed solution features an axial signal that integrates to 20% of the possible spins, indicating formation of some Cu(II)-containing products. However, it appears that the sample decomposition is a complex process, as isolation of the organic products after decomposition and subsequent GC/MS analysis reveals the formation of over 25 different species (data not shown). Thus, it appears that the decomposition proceeds via multiple pathways, none of which have been definitively characterized.

Resonance Raman spectra of the yellow-green intermediate were collected using 406.7 nm excitation. While a large number of resonance-enhanced peaks are observed, only one is isotope sensitive (Figure 3). The complex prepared with ¹⁶O₂ exhibits a spectrum with a peak at 974 cm⁻¹ that shifts to 908 cm⁻¹ when ¹⁸O₂ is used, consistent with its assignment as an O−O stretching vibration (Δ(¹⁸O) = 66 cm⁻¹; calcd for O−O harmonic oscillator, 56 cm⁻¹). These values are quite similar to those reported for the side-on 1:1 Cu−O₂ adducts of the β-diketiminate ligands that have considerable Cu(III)−peroxo character (e.g., 968 cm⁻¹, Δ(¹⁸O) = 51 cm⁻¹),[14] as well as one other 1:1 Cu−O₂ complex characterized by FTIR spectroscopy,[8] but are much lower than values reported for other 1:1 Cu−O₂ adducts considered to be Cu(II)−superoxo complexes (1112−1122 cm⁻¹).[9,10,13,44]

(44) Jazdzewski, B. A.; Reynolds, A. M.; Holland, P. L.; Young, V. G., Jr.; Kaderli, S.; Zuberbühler, A. D.; Tolman, W. B. *J. Biol. Inorg. Chem.* **2003**, *8*, 381.
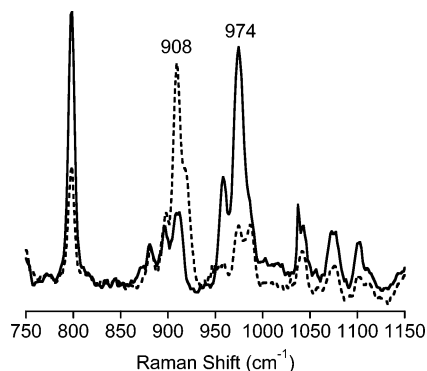
Figure 3. Resonance Raman spectra (λ_{ex} = 406.7 nm, −196 °C) of acetone solutions of the intermediate resulting from the reaction of $L^2Cu(MeCN)$ with $^{16}O_2$ (solid line) or $^{18}O_2$ (dashed line).
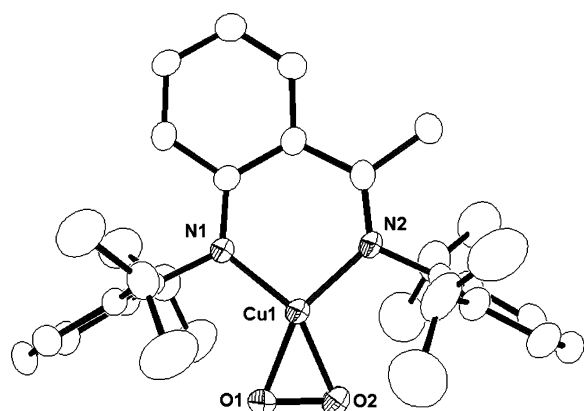

Figure 4. X-ray crystal structure of L^2CuO_2, with all non-hydrogen atoms shown as 50% thermal ellipsoids.

X-ray-quality crystals of L^2CuO_2 were grown at −80 °C from a mixture of diethyl ether, pentane, and acetone; selected bond distances and angles are listed in Table 1, and crystallographic data are given in Table S1. As shown in Figure 4, the complex features side-on coordination of the bound O_2 similar to that of the previously reported complex supported by a β-diketiminate ligand.[14] This structure is of significantly higher quality, however, and unlike the β-diketiminate case where the O−O bond is generated by a symmetry operation and the molecule is disordered in the crystal, the asymmetric unit for L^2CuO_2 contains a full molecule and there is no disorder in the complex itself. Thus, the structure provides quite precise bond distances and angles (Table 1). Notably, the O−O bond length is 1.392(2) Å, which closely agrees with the value determined for the β-diketiminate complex and is similarly indicative of significant Cu(III)−peroxo character.[11,14] In addition, Δ_{Cu-N} = 0.037 Å, a degree of asymmetry in the binding of L^2 to the copper center that is decreased compared to that seen in $L^2Cu(MeCN)$, as well as other transition-metal complexes of anilido imine ligands, which have Δ_{M-N} values of up to 0.35 Å.[19,20] These differences are typically attributed to the formal charge difference of the two N donors. The reason for the increased symmetry in L^2CuO_2 remains unclear. Interestingly, despite the large difference in the Δ_{Cu-N} values, the differences in the remaining bond lengths of the six-membered chelate are small in both $L^2Cu(MeCN)$ and L^2CuO_2. Specifically, Δ_{C-N} = 0.047 Å for $L^2Cu(MeCN)$ and 0.045 Å for L^2CuO_2, and
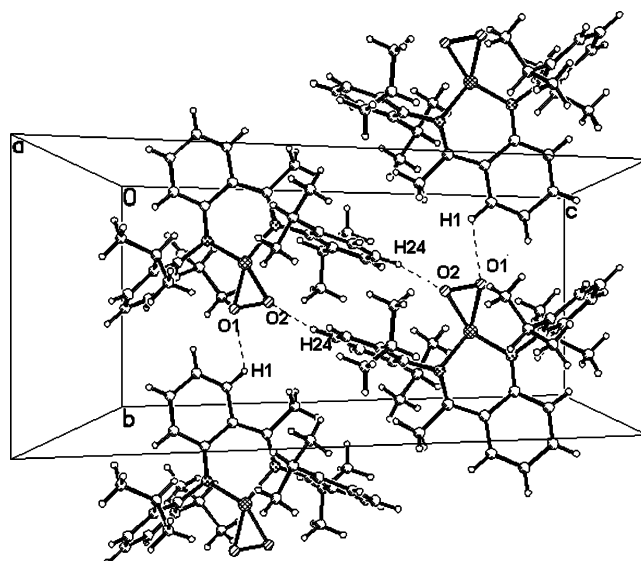

Figure 5. Packing diagram of the X-ray crystal structure of L^2CuO_2 highlighting the interactions between O1 and H1 and between O2 and H24.
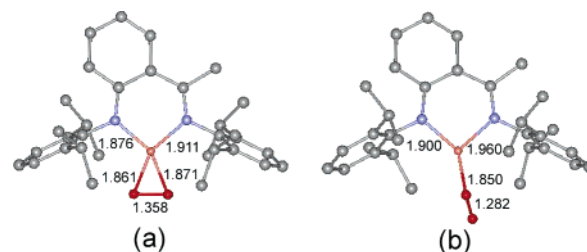

Figure 6. Optimized geometries of L^2CuO_2 singlets with the O_2 moiety coordinated (a) side-on and (b) end-on. Hydrogen atoms are omitted for clarity. Selected bond distances (Å) are reported. Gray represents C, blue N, red O, and pink Cu.

Δ_{C-C} = 0.019 Å in $L^2Cu(MeCN)$ and 0.024 Å in L^2CuO_2. These degrees of bond alternation are also smaller than those observed in many other anilido imine systems, consistent with greater charge delocalization in the copper complexes.

Finally, inspection of crystal packing diagrams (Figure 5) reveals interactions between the oxygen atoms of the coordinated O_2 moiety and aromatic hydrogen atoms on neighboring molecules; O1 lies 2.537 Å from H1 of another complex, while O2 lies 2.397 Å from H24 of a third molecule. While these evidently weak interactions are notable,[45] they are not likely to significantly influence the coordination geometry of the complex.

Dioxygen Reactivity (Theory). In accord with the structure found experimentally and determined to be EPR silent, theoretical calculations predict the side-on singlet state of L^2CuO_2 (Figure 6a) to have the lowest energy among the end-on and side-on singlet and triplet possibilities. In particular, it is 3.5 kcal mol⁻¹ more stable than the end-on singlet (Figure 6b), and has a free energy lower by 14.1 and 19.4 kcal mol⁻¹ than those of the side-on and end-on triplets, respectively. The side-on singlet features an O−O bond length of 1.358 Å, which is in reasonable agreement with

---

(45) Musah, R. A.; Jensen, G. M.; Rosenfeld, R. J.; McRee, D. E.; Goodin, D. B. *J. Am. Chem. Soc.* **1997**, *119*, 9083 and references cited in Figure S2.

Table 2. Mulliken Charge Populations for $L^2Cu(MeCN)$ and the Singlet Forms of $L^2CuO_2{}^a$

	Cu	O1	O2	L^2
$L^2Cu(MeCN)$	0.35	0.00	0.00	−0.43
end-on singlet	0.51	−0.22	−0.14	−0.15
side-on singlet	0.70	−0.27	−0.27	−0.16

^{a} The oxygen atom closest to Cu is labeled O1.

Table 3. Computed and Experimentally Determined $\nu(O-O)$ (cm^{-1}) for the Singlet Forms of $L^2CuO_2{}^a$

	$^{16}O-^{16}O$	$^{18}O-^{16}O$	$^{16}O-^{18}O$	$^{18}O-^{18}O$
computed end-on	1226	1198	1198	1158
computed side-on	1041	1012	1012	983
experimental	974	n/a	n/a	908

^{a} In each case, the first oxygen atom listed is the one closest to Cu.

the 1.39 Å distance in the crystal structure.[46] Similarly small differences are seen between the calculated and crystallographically determined Cu−O distances, and the optimized structure as a whole has an RMS deviation of 0.188 Å versus the crystal geometry. The Cu−O and Cu−N bond length differentials of 0.04−0.05 Å between computed and crystal structures for L^2CuO_2 can be attributed to the gas-phase nature of the geometry optimization, which tends to exhibit less charge separation than the condensed-phase (i.e., crystal) structure, leading to relatively looser binding between Cu and the anilido imine ligand and O_2. The effect is small, however, as evidenced by the nominal difference in bond lengths and the flatness of the potential energy curves within that range in bond lengths.

Mulliken charge populations (Table 2) reveal that oxidation of both Cu and the anilido imine ligand accompanies reduction of dioxygen upon adduct formation. In both the end-on and side-on singlet structures, the transfer of electron density from the anionic ligand serves to stabilize the oxidized Cu and promotes activation of dioxygen. Oxidation of the ligand is nonetheless limited to ∼0.25 au, with the additional reduction of the dioxygen moiety in the side-on versus end-on structure being nearly entirely tied to Cu oxidation.

Computed vibrational frequencies (Table 3) show that $\nu(^{16}O_2)$ for the side-on singlet state of L^2CuO_2 is consistent with the value obtained from resonance Raman spectroscopy. Further agreement between theory and experiment can be seen in the $\Delta\nu(^{18}O_2)$ value (58 cm^{-1} by DFT and 66 cm^{-1} from resonance Raman). Consistent with the nearly symmetric O_2 coordination in the singlet side-on structure, the $\nu(O_2)$ values for the mixed-label isotopomers are essentially equal. Interestingly, $\Delta\nu(O_2)$ between the mixed-label isotopomers in the case of end-on dioxygen coordination is also approximately zero. This result is consistent with previous conclusions that discrimination between end-on and side-on coordination via mixed-label experiments is problematic.[10,47]

Taken together, the geometric, electronic, and vibrational data calculated for the side-on singlet L^2CuO_2 support a formulation intermediate between the Cu(II)−superoxo and Cu(III)−peroxo extremes but lying closer to the peroxo side of the continuum.[11a,12] In addition to the O−O bond length in the side-on structure, the average Cu−N (1.845 Å, crystal; 1.893 Å, theoretical) bond length is less than those observed on average in other 4-coordinate compounds of Cu(II) or Cu(III) supported by β-diketiminate ligands,[14c] implying considerable Cu(III)−peroxo character in the current η^2 1:1 Cu−O_2 adduct. Further evidence is provided by the orbital occupation numbers (Figure S3 in the Supporting Information) from the multiconfigurational CASPT2 calculations, which show Cu to be closer to d^8 than d^9 and dioxygen to be closer to $O_2{}^{2-}$ than $O_2{}^-$ in the singlet side-on structure. Computed and experimental $\nu(O-O)$ values (Table 3) likewise fall between the well-established typical values for O−O stretching frequencies of 1075−1200 cm^{-1} for superoxo ligands and 790−930 cm^{-1} for peroxo ligands.[48]

These conclusions are closely analogous to those offered previously for the analogous O_2 adducts supported by the β-diketiminate ligands.[11a,12,14] Particularly notable is the similarly symmetric coordination of O_2 to the Cu centers in these two systems, despite the differences in steric and electronic properties of the β-diketiminate and anilido imine ligands, such as the formal charge difference of one unit between the two N atoms in the latter. The relative energies of the singlet η^1 and η^2 isomers of the 1:1 Cu−O_2 adducts for the two ligand systems are also nearly identical, and preliminary calculations indicate that the mechanisms and energetics of their respective dioxygen activation processes are also completely analogous.[14c,49]

However, in contrast to the β-diketiminate system, it was not sufficient in the present case to employ a polarized double-ζ basis set (in the case of Cu, a DZP basis for the valence electrons) in the CASPT2 calculations to obtain energies in accord with experimental data. Using a DZP basis in the present case of the anilido imine ligand led to an erroneous prediction (in light of the crystallographic data) that the end-on singlet was the lowest energy 1:1 Cu−O_2 adduct. By expanding the basis to the TZP level for the most chemically reactive portion of the molecule, namely, Cu (for the valence electrons), N, O, and H atoms bonded to nitrogen, while decreasing the basis set size on the remainder of the molecule for computational tractability, a proper ordering of the energies with the side-on singlet as the most stable structure was recovered. The computations with the TZP basis are consistent with the tendency of the more complete basis set to provide an improved stabilization of internal charge separation,[50] as the more Cu(III)−peroxo-like side-on structure is determined to be lower in energy than the more Cu(II)−superoxo-like end-on form, versus the opposite result when the all-DZP basis was used. Specifically, use of the TZP basis stabilizes the end-on singlet by 3.2 kcal mol^{-1} versus that of the DZP basis, the side-on singlet by 15.4 kcal mol^{-1}. This charge stabilization effect arises in the anilido imine system due to the asymmetric ligation of the Cu center

(46) Geometries for the computed triplets are presented in Figure S2.
(47) Kinsinger, C. R.; Gherman, B. F.; Gagliardi, L.; Cramer, C. J. *J. Biol. Inorg. Chem.*, in press.

(48) Vaska, L. *Acc. Chem. Res.* **1976**, *9*, 175.
(49) Gherman, B. F.; Tolman, W. B.; Cramer, C. J. To be published.
(50) Gherman, B. F.; Goldberg, S. D.; Cornish, V. W.; Friesner, R. A. *J. Am. Chem. Soc.* **2004**, *126*, 7652.

which is composed in part of an amide nitrogen atom bearing a formal negative charge. The negative charge on the β-diketiminate ligand, in contrast, is fully conjugated along the ligand backbone, resulting in each ligating nitrogen atom formally bearing considerably less than one unit of negative charge. The charge differential, consequently, between the Cu center and the N atoms in the anilido imine ligand case is larger than in the β-diketiminate ligand case (Table S2 in the Supporting Information), necessitating the use of the TZP basis for the former. The TZP basis is particularly essential in predicting the proper stability of the side-on singlet, where this charge differential is most pronounced.

Conclusions

Copper(I) complexes of the anilido amine ligands L^1 and L^2 have been prepared and their low-temperature reactivities with O_2 explored. In the case of the complex supported by L^2, characterization by UV−vis, EPR, and resonance Raman spectroscopy, X-ray crystallography, and theoretical calculations has led to formulation of the oxygenation product as a singlet side-on complex, L^2CuO_2, with significant Cu(III)−peroxo character. Of particular note is the quality of the X-ray structure, which has enabled the highest resolution definition of a mononuclear CuO_2 moiety available to date. The observation of symmetric side-on O_2 binding closely analogous to that observed in systems comprising β-diketiminate ligands suggests that more asymmetric coordination of O_2 (e.g., end-on) will require imposition of greater electronic and/or steric asymmetry than present in the anilido imine L^2. Modulation of the electron-donating characteristics of the supporting ligands may also be necessary to achieve end-on O_2 binding. Ultimately, through an understanding of such requirements, important insights into ligand structural influences on the properties of mononuclear Cu−O₂ intermediates relevant to biology and catalysis will be obtained.

Supporting Information Available: Supplementary Tables S1 and S2 and Figures S1−S3, including X-ray crystallographic data (CIF) and a packing diagram for $L^2Cu(MeCN)$ and atomic coordinates and vibrational frequencies for all computed model L^2 structures (PDF). This material is available free of charge via the Internet at http://pubs.acs.org.

IC050280P